

Technical report 13-017

Integrated Urban Traffic Control for the Reduction of Travel Delays and Emissions*

S. Lin, B. De Schutter, Y. Xi, and H. Hellendoorn

To cite this work, please refer to the published version:

S. Lin, B. De Schutter, Y. Xi, and H. Hellendoorn, “Integrated urban traffic control for the reduction of travel delays and emissions,” *IEEE Transactions on Intelligent Transportation Systems*, vol. 14, no. 4, pp. 1609–1619, Dec. 2013. doi:[10.1109/TITS.2013.2263843](https://doi.org/10.1109/TITS.2013.2263843)

Delft Center for Systems and Control
Delft University of Technology
Mekelweg 2, 2628 CD Delft
The Netherlands
phone: +31-15-278.24.73 (secretary)
URL: <https://www.dcsc.tudelft.nl>

* This report can also be downloaded via <https://dpub.eu/13-017>

Integrated urban traffic control for the reduction of travel delays and emissions

Shu Lin, *Member, IEEE*, Bart De Schutter, *Senior Member, IEEE*, Yugeng Xi, *Senior Member, IEEE*,
and Hans Hellendoorn

Abstract—Refining transportation mobility and improving the living environment are two important issues that need to be addressed in urban traffic. In order to reduce traffic delays as well as traffic emissions for urban traffic networks, this paper first proposes an integrated macroscopic traffic model that integrates a macroscopic urban traffic flow model with a microscopic traffic emission model for individual vehicles. This integrated model is able to predict the traffic flow states, as well as the emissions released by every vehicle at different operational conditions, i.e. the speed and the acceleration. Then, Model Predictive Control is applied to control urban traffic networks based on this integrated traffic model, aiming at reducing both travel delays and traffic emissions of different gases. Finally, simulations are performed to assess this multi-objective control approach. The obtained simulation results illustrate the control effects of the model predictive controller.

Index Terms—Urban traffic network control, Model predictive control, Urban traffic modeling.

I. INTRODUCTION

TRAFFIC emissions is one of the biggest sources of the environmental pollution in cities. The emissions of vehicles contain several harmful substances, such as nitrogen oxides (NO_x , i.e. nitrogen monoxide, nitrogen dioxide), hydrocarbons (HC), carbon monoxide (CO), carbon dioxide (CO_2), and fine particulate matter. Around the world, approximately 50% of the NO_x emission, and 90% of the CO emission come from traffic [1]. These emissions can pollute the air that people breathing, cause smog for cities, do harm to soil, water, buildings, etc. In general, traffic pollution deteriorates our living environment, and increases the risk for people who have heart or lung diseases. Therefore, it is necessary to integrate traffic emission control into the urban traffic management system, so as to provide a healthier, safer, and more comfortable living environment for people in urban areas.

For most of the existing traffic control strategies, the control objectives are economy-oriented: they are mainly focusing on reducing traffic delays, travel time, and traffic congestion, and on improving the traffic flow throughput. For instance, SCATS [2] aims at reducing the traffic occupancy in front of the traffic signals; SCOOT [3] mainly focuses on controlling the length of queues; The total time spent or total travel delays is

usually taken as the control objective in many optimization-based traffic control strategies [4]–[12]. Since traffic emissions have a significant influence on air, climate, and human health, it is not a sustainable policy to only consider economy-oriented performance criteria for traffic control strategies. Consequently, traffic emissions, as an environment-oriented traffic control objective, draws more attention [13]–[19].

In the aforementioned research works taking traffic emissions as control objectives, traffic emissions are controlled from two points of view: intelligent-vehicle-based methods and traffic-management-based methods. Intelligent-vehicle-based methods implement cruise control function to vehicles by adopting vehicle-to-vehicle or infrastructure-to-vehicle communication technologies, so as to get a fuel efficient and reduced emission driving behavior. Adaptive cruise control algorithms were proposed adopting upcoming road infrastructure information (e.g. traffic signals) so as to smooth traffic flows, and thus to reduce fuel consumptions [13], [14]. A vehicular network with virtual traffic lights was proposed in [20], which can improve the utilization efficiency of an intersection, and was proved to have good effect on reducing CO_2 emission [15]. Due to the use of information of neighboring vehicles and infrastructures (e.g. traffic lights), intelligent-vehicle-based method opens a way to help drivers have more optimal driving behaviors, and consequently to decrease the emission level of a traffic network. However, the intelligent-vehicle-based method focuses more on the individual vehicles and is often under a decentralized control structure, therefore it lacks a global regulation and control of entire traffic networks. On the contrary, traffic-management-based method can control and optimize traffic control measures to smooth and schedule traffic flows, and balance traffic emissions within traffic networks. Traffic control strategies were proposed for traffic emission reduction based on the traffic flow information collected from in-vehicle information broadcasting devices [16]. Stevanovic et al. [17] integrated a microscopic traffic simulator, a microscopic emission model, and a signal optimization tool together to search for the best traffic signal timings for fuel consumption and emission reduction. This research established an effective tool for off-line optimization of the traffic signals for vehicular emission mitigation. Zegeye et al. [18], [19] designed model predictive control strategies to online control both the total travel time and the total emissions, based on an integrated model of a macroscopic traffic flow model and a microscopic traffic emission model. But this control strategy is only for freeway traffic networks. For urban traffic networks, there is still lacking of efficient and effective traffic control strategy for reduction of both travel delays and emissions.

S. Lin is with School of Computer and Control Engineering, University of Chinese Academy of Sciences, Beijing, China. Y. Xi and S. Lin are with Department of Automation, Shanghai Jiao Tong University, and Key Laboratory of System Control and Information Processing, Ministry of Education of China. lisashulin@gmail.com, ygxi@sjtu.edu.cn

B. De Schutter, and J. Hellendoorn are with the Delft Center for Systems and Control, Delft University of Technology, The Netherlands. [b.deschutter](mailto:b.deschutter@tudelft.nl), [j.hellendoorn](mailto:j.hellendoorn@tudelft.nl)

Manuscript received May, 2013

Therefore, in this paper, a model predictive control (MPC) control strategy is proposed considering both traffic delays and emissions of traffic networks. As a model-based optimization control approach, MPC [21] is an advanced control method that can globally coordinate traffic network flows, and can easily combine multiple objectives into one control problem. An integrated traffic model is established for the MPC controller to predict/estimate both the travel delays and the traffic emissions of traffic networks. Since an MPC controller needs to optimize the control performance in a receding horizon way, it has a high requirement for online computation efficiency. Thereafter, the prediction model of the MPC controller has to keep efficient to satisfy online computing requirement. The proposed integrated traffic flow and emission model combines a macroscopic urban traffic flow model (i.e. the S model [22]) with a microscopic traffic emission model (i.e. the VT-micro model [23]). The VT-micro model can give a comparatively accurate estimate of the vehicular emissions based on the operational conditions of the vehicles, i.e. velocity and acceleration. The S model is proved to be a fast and accurate macroscopic traffic flow model for MPC control purposes. The integrated traffic flow and emission model keeps the advantages of the two models, and is able to provide reasonable estimates of both travel delays and emissions for the MPC controller.

This paper is organized as follows. Section II and III briefly introduce a macroscopic urban traffic flow model (S model) and a microscopic vehicle emission model (VT-micro). Section IV describes the integrated traffic flow and emission model. The MPC controller design is given in Section V. Section VI presents the results, and Section VII concludes the paper.

II. MACROSCOPIC URBAN TRAFFIC MODEL (S MODEL)

In the macroscopic urban traffic model of [22], called the S model, we define J the set of nodes (intersections), and L the set of links (roads) in the urban traffic network. A link (u, d) is marked by its upstream node u ($u \in J$) and downstream node d ($d \in J$). The input and output links of link (u, d) can be also specified by these upstream and downstream nodes. The sets of input and output nodes for link (u, d) are $I_{u,d} \subset J$ and $O_{u,d} \subset J$. Some variables are first defined as (see Fig. 1):

- $I_{u,d}$: set of input nodes of link (u, d) ,
- $O_{u,d}$: set of output nodes of link (u, d) ,
- k_d : simulation step counter,
- c_d : cycle time for intersection d ,
- $n_{u,d}(k_d)$: number of vehicles in link (u, d) at step k_d ,
- $q_{u,d}(k_d)$: queue length at step k_d in link (u, d) (in number of vehicles); $q_{u,d,o}$ is the queue length of the sub-stream turning to link o ,
- $\alpha_{u,d}^{\text{leave}}(k_d)$: flow rate leaving link (u, d) at step k_d ; $\alpha_{u,d,o}^{\text{leave}}(k_d)$ is the leaving flow rate of the sub-stream towards o ,
- $\alpha_{i,u,d}^{\text{leave,cont}}(t)$ the continuous-time leaving flow rate from the upstream link i of link (u, d) ($i \in I_{u,d}$),
- $\alpha_{u,d}^{\text{arriv}}(k_d)$: flow rate arriving at the end of the queue in link (u, d) at step k_d ; $\alpha_{u,d,o}^{\text{arriv}}(k_d)$ is the arriving flow rate of the sub-stream towards o ,

- $\alpha_{u,d}^{\text{enter}}(k_d)$: flow rate entering link (u, d) at step k_d ;
- $\alpha_{i,u,d}^{\text{enter}}(k_d)$ is the flow rate entering link (u, d) from i ,
- $\beta_{u,d,o}(k_d)$: relative fraction of the traffic on link (u, d) turning to o at step k_d ,
- $\mu_{u,d}$: saturated flow rate leaving link (u, d) ,
- $g_{u,d,o}(k_d)$: green time length during step k_d for the traffic stream towards o in link (u, d) ,
- $v_{u,d}^{\text{free}}$: free-flow vehicle speed in link (u, d) ,
- $C_{u,d}$: capacity of link (u, d) expressed in number of vehicles,
- $L_{u,d}^{\text{lane}}$: number of lanes in link (u, d) ,
- $\Delta c_{u,d}$: cycle time offset between node u and node d ,
- l_{veh} : average vehicle length.

In the S model, every intersection takes the cycle time as its simulation time interval. The cycle times for intersections u and d , which are denoted by c_u and c_d respectively, can be different from each other. In this situation, the simulation step counters of different intersections are not same. As cycle times are the simulation time intervals of the S model, the input and output flow rates of the link are averaged over the cycle times in the S model.

Taking the cycle time c_d as the length of the simulation time interval for link (u, d) and k_d as the corresponding time step counter, the number of the vehicles in link (u, d) is updated according to the input and output flow rate over c_d :

$$n_{u,d}(k_d + 1) = n_{u,d}(k_d) + \left(\alpha_{u,d}^{\text{enter}}(k_d) - \alpha_{u,d}^{\text{leave}}(k_d) \right) \cdot c_d . \quad (1)$$

The leaving flow rate $\alpha_{u,d}^{\text{leave}}(k_d)$ is the sum of the leaving flow rates $\alpha_{u,d,o}^{\text{leave}}(k_d)$ turning to each output link $o \in O_{u,d}$.

The average leaving flow rate over c_d is determined by the capacity of the intersection, the number of cars waiting and arriving, and the available space in the downstream link:

$$\alpha_{u,d,o}^{\text{leave}}(k_d) = \min \left(\beta_{u,d,o}(k_d) \cdot \mu_{u,d} \cdot g_{u,d,o}(k_d) / c_d, \right. \\ \left. q_{u,d,o}(k_d) / c_d + \alpha_{u,d,o}^{\text{arriv}}(k_d), \right. \\ \left. \beta_{u,d,o}(k_d) (C_{d,o} - n_{d,o}(k_d)) / c_d \right) . \quad (2)$$

The number of vehicles waiting in the queue turning to link o is updated as

$$q_{u,d,o}(k_d + 1) = q_{u,d,o}(k_d) + \left(\alpha_{u,d,o}^{\text{arriv}}(k_d) - \alpha_{u,d,o}^{\text{leave}}(k_d) \right) \cdot c_d . \quad (3)$$

The flow of vehicles that entered link (u, d) will arrive at the end of the queues after a time delay $\tau(k_d) \cdot c_d + \gamma(k_d)$:

$$\alpha_{u,d}^{\text{arriv}}(k_d) = \frac{c_d - \gamma(k_d)}{c_d} \alpha_{u,d}^{\text{enter}}(k_d - \tau(k_d)) + \\ \frac{\gamma(k_d)}{c_d} \alpha_{u,d}^{\text{enter}}(k_d - \tau(k_d) - 1), \quad (4)$$

with

$$\tau(k_d) = \text{floor} \left\{ \frac{(C_{u,d} - q_{u,d}(k_d)) \cdot l_{\text{veh}}}{L_{u,d}^{\text{lane}} \cdot v_{u,d}^{\text{free}} \cdot c_d} \right\}, \\ \gamma(k_d) = \text{rem} \left\{ \frac{(C_{u,d} - q_{u,d}(k_d)) \cdot l_{\text{veh}}}{L_{u,d}^{\text{lane}} \cdot v_{u,d}^{\text{free}} \cdot c_d} \right\}. \quad (5)$$

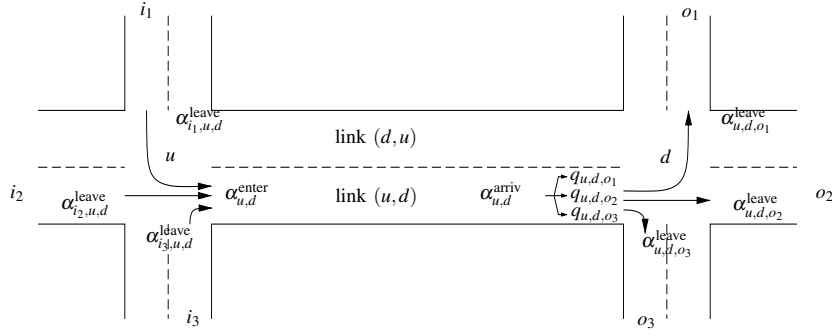


Fig. 1. A link connecting two traffic-signal-controlled intersections

When reaching the end of the link, the arriving flow rate is separated into sub-streams by multiplying it with the turning rate $\beta_{u,d,o}(k_d)$.

The flow rate entering link (u,d) is the sum of the flow rates entering from all the upstream links:

$$\alpha_{u,d}^{\text{enter}}(k_d) = \sum_{i \in I_{u,d}} \alpha_{i,u,d}^{\text{enter}}(k_d) = \sum_{i \in I_{u,d}} \alpha_{i,u,d}^{\text{leave}}(k_u). \quad (6)$$

Some operations need to be carried out to synchronize the leaving and entering flow rates. This goes as follows: A common control time interval is adopted by all the intersections in the network, as

$$T_{\text{ctrl}} = a_j \cdot c_j, \quad \text{for all } j \in J, \text{ with } a_j \text{ an integer}, \quad (7)$$

where T_{ctrl} is the least common multiple of all the intersection cycle times in the traffic network.

The leaving flow rates in the timing of intersection u can be recast into the entering flow rates in the timing of intersection d as follows. First, we transform the discrete-time leaving flow rates from the upstream links into continuous time using a zero-order hold strategy, as

$$\alpha_{i,u,d}^{\text{leave,cont}}(t) = \alpha_{i,u,d}^{\text{leave}}(k_u), \quad k_u \cdot c_u \leq t < (k_u + 1) \cdot c_u. \quad (8)$$

Then, we convert the result again to obtain the average entering flow rates in time step k_d :

$$\alpha_{i,u,d}^{\text{enter}}(k_d) = \frac{\int_{k_d \cdot c_d + \Delta c_{u,d}}^{(k_d+1) \cdot c_d + \Delta c_{u,d}} \alpha_{i,u,d}^{\text{leave,cont}}(t) dt}{c_d}. \quad (9)$$

We refer the interested readers to [22] for more details about the S model.

III. MICROSCOPIC TRAFFIC EMISSION MODEL

The operating conditions of vehicles, e.g. speed, acceleration, and engine load, are the most decisive elements for the emission of harmful substances. Therefore, traffic emission models are established based on the operating conditions of vehicles. Average-speed-based models calculate the emissions of each vehicle based on the average traveling speed of the vehicle. This average traveling speed can be calculated either over the entire trip, or over some local time periods to take some variations of the speed into consideration [24]. However, the emissions of a vehicle do not only depend on the speed but also on the acceleration and the deceleration of the vehicle.

On signalized urban roads, the acceleration and deceleration are vehicle dynamics that cannot be ignored. Therefore, it is better to select dynamic emission models, which use more detailed knowledge of the vehicle dynamics, e.g. the speed and acceleration data of each vehicle at every time step. As microscopic traffic emission models, dynamic models yield more accurate estimates of the vehicle emissions than the average-speed-based models, and are more suitable for urban road networks.

VT-micro [23] is a microscopic dynamic traffic emission model. It evaluates the emissions based on not only the speed of every vehicle, but also the acceleration or the deceleration of each vehicle. VT-micro generates emissions of an individual vehicle with index i at every time step k based on the current speed $v_i(k)$ and acceleration $a_i(k)$ of the vehicle, as

$$E_{\theta,i}(v_i(k), a_i(k)) = \exp(\tilde{\mathbf{v}}_i^T(k) \mathbf{P}_\theta \tilde{\mathbf{a}}_i(k)), \quad (10)$$

where $E_{\theta,i}$ stands for the emission for $\theta \in M = \{\text{CO}, \text{NO}_x, \text{HC}\}$; $\tilde{\mathbf{v}}_i(k)$ and $\tilde{\mathbf{a}}_i(k)$ are defined as vectors, $\tilde{\mathbf{v}}_i(k) = [1 \ v_i(k) \ v_i^2(k) \ v_i^3(k)]^T$, $\tilde{\mathbf{a}}_i(k) = [1 \ a_i(k) \ a_i^2(k) \ a_i^3(k)]^T$, with the elements formed by the speed and the acceleration of vehicle i with different exponents; and \mathbf{P}_θ is the pre-calibrated parameter matrix of the model for different types of emissions. The matrices \mathbf{P}_θ for $\theta \in M$ can be found in [23].

IV. INTEGRATED TRAFFIC FLOW AND TRAFFIC EMISSION MODEL

A. Urban traffic behaviors for individual vehicles

As a microscopic model, the VT-micro model provides the emissions of an individual vehicle at a certain location and a certain time instant. But, as a macroscopic model, the S model only provides information of traffic flows instead of every detail of every individual vehicle. However, the S model can capture the main behavior of the vehicles, when they are running along a road. The time period spent by a vehicle running along a road can be divided into several parts, in each of which the behavior of the vehicle is assumed to be uniform. Define the set of the behaviors as $B = \{\text{free}, \text{idling}, \text{dec}, \text{acc}, \text{nonstop}, \text{sns}\}$, where dec stands for deceleration, acc stands for acceleration, and sns stands for start-and-stop behavior. Fig. 2 shows how the velocity of a vehicle could vary in different behavior regions, when it travels along an urban road.

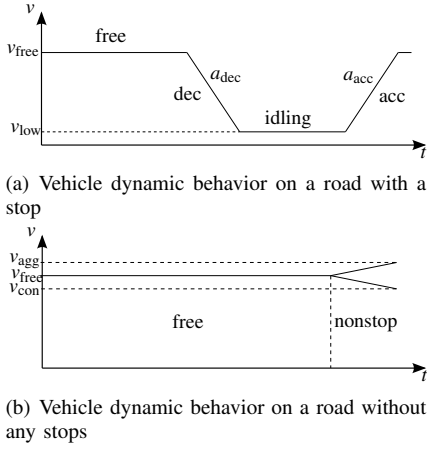


Fig. 2. Vehicle dynamic behavior on a road

As Fig. 2(a) shows, in the regions “free” and “idling”, the vehicle runs with a constant velocity, i.e. the acceleration is $a = 0$. The region “free” stands for the time period that the vehicle is running on the link with free-flow speed $v = v_{\text{free}}$, while the region “idling” represents the time period that the vehicle is moving in a queue in front of an intersection with a very low speed $v = v_{\text{low}}$. Therefore, the emission functions for the vehicle running with free-flow speed and the vehicle idling with a very low speed in the queues are respectively

$$E_{\theta,i}^{\text{free}}(k) = E_{\theta,i}(v_{\text{free}}, 0), \quad (11)$$

$$E_{\theta,i}^{\text{idling}}(k) = E_{\theta,i}(v_{\text{low}}, 0). \quad (12)$$

The regions “dec” and “acc” represent the deceleration and acceleration behavior of the vehicle near an intersection respectively. Here, the assumption is made that the vehicle will decelerate and accelerate with a constant acceleration $a_{\text{dec}} < 0$ and $a_{\text{acc}} > 0$ respectively. The emission functions for the vehicle decelerating and accelerating are

$$E_{\theta,i}^{\text{dec}}(k) = -\frac{a_{\text{dec}}}{v_{\text{low}} - v_{\text{free}}} \int_{v_{\text{free}}}^{v_{\text{low}}} E_{\theta,i}(v, a_{\text{dec}}) dv, \quad (13)$$

$$E_{\theta,i}^{\text{acc}}(k) = \frac{a_{\text{acc}}}{v_{\text{free}} - v_{\text{low}}} \int_{v_{\text{low}}}^{v_{\text{free}}} E_{\theta,i}(v, a_{\text{acc}}) dv, \quad (14)$$

which are the average released emissions over the time when vehicles are accelerating and decelerating.

If the vehicle arrives at the stop line, where no queue is in front of it and the traffic light is also green, then the vehicle will leave the link without a stop. In such situation, the behavior of drivers can be roughly classified in two categories: 1) aggressive behavior, i.e. accelerating slightly in order to pass the intersection within the green light; 2) conservative behavior, i.e. decelerating a little bit so as to pass the intersection safely. In general, if the arriving traffic density is low (e.g. very few vehicles), drivers tend to have the aggressive behavior; if the arriving traffic density is high, drivers tend to have the conservative behavior. Therefore, the

emissions for the nonstop vehicles are (see Fig. 2(b))

$$E_{\theta,i}^{\text{nonstop}}(k) = \begin{cases} \frac{a_{\text{acc}}}{v_{\text{agg}} - v_{\text{free}}} \int_{v_{\text{free}}}^{v_{\text{agg}}} E_{\theta,i}(v, a_{\text{acc}}) dv & \text{if } O \leq \lambda \\ -\frac{a_{\text{dec}}}{v_{\text{con}} - v_{\text{free}}} \int_{v_{\text{free}}}^{v_{\text{con}}} E_{\theta,i}(v, a_{\text{dec}}) dv & \text{if } O > \lambda \end{cases}, \quad (15)$$

where the less conservative drivers will speed up to $v_{\text{agg}} (> v_{\text{free}})$, the more conservative drivers will decrease their speed to $v_{\text{con}} (< v_{\text{free}})$, $O = \alpha_{u,d}^{\text{arriv}}(k_d) / \mu_{u,d}$ ($kT \in [c_d \cdot k_d, c_d \cdot (k_d + 1)]$) is defined as the capacity occupancy rate of a link (i.e. the arriving traffic flow rate divides the saturation flow rate of the link), and $\lambda \in [0, 1]$ is the threshold.

When the traffic in a link is saturated, there are vehicles arriving at the link, but that cannot leave the link within the same cycle. These vehicles have to accelerate and then decelerate to keep on waiting in queues, which we call start-and-stop behavior. The emissions for the start-and-stop vehicles can be estimate as

$$E_{\theta,i}^{\text{sns}}(k) = \frac{a_{\text{acc}} a_{\text{dec}}}{a_{\text{dec}}(v_{\text{sns}} - v_{\text{low}}) + a_{\text{acc}}(v_{\text{low}} - v_{\text{sns}})} \int_{v_{\text{low}}}^{v_{\text{sns}}} (E_{\theta,i}(v, a_{\text{acc}}) + E_{\theta,i}(v, a_{\text{dec}})) dv, \quad (16)$$

where v_{sns} is the speed that a vehicle reaches when it is subject to a start-and-stop behavior in waiting queues.

Remark 1: In this subsection, for the sake of simplicity of the explanation, all the variables are assumed to be the same for a vehicle on any link. If the locations of vehicles are considered, then the emission $E_{\theta,i}^b$ ($\theta \in M$) of vehicle i on link (u, d) in behavior b should be remarked as $E_{\theta,u,d,i}^b$.

B. Integrated VT-S traffic emission model

The S model provides macroscopic traffic states for each link $(u, d) \in L$ in each simulation time interval (cycle time). The traffic states include the number of vehicles traveling with free-flow speed, the number of vehicles decelerating and accelerating, and the number of vehicle waiting and idling in queues. The vehicles idling in front of the stop-line in link (u, d) can be classified into four groups:

- *Idling,1:* Vehicles idling for the rest of the cycle time after deceleration;
- *Idling,2:* Vehicles idling between deceleration and acceleration;
- *Idling,3:* Vehicles idling for the entire cycle time;
- *Idling,4:* Vehicles idling from the start of the cycle time until acceleration.

Correspondingly, the VT-micro model can provide an estimate of the emissions for the vehicles under these traffic states as Section IV-A shows. By summing up the emissions of vehicles in different traffic states provided by the S model, the total emission of a road network can be calculated.

Based on the traffic flow state information and the vehicle emission information, a macroscopic traffic emission model can be obtained by combining the macroscopic S model and the VT-micro model together, which results in a macroscopic integrated traffic flow and emission model, which we call the VT-S model.

The VT-S model for emission $\theta \in M$ in link $(u, d) \in L$ during time period $[c_d \cdot k_d, c_d \cdot (k_d + 1)]$ is

$$\begin{aligned} E_{\theta, u, d}(k_d) &= \sum_{b \in B} \sum_{k \in \mathcal{K}(d, k_d)} T \cdot \sum_{i \in \mathcal{V}(b, u, d, k)} E_{\theta, u, d, i}^b(k) \\ &= \sum_{b \in B} E_{\theta, u, d}^b(k_d) \cdot N_{u, d}^b(k_d) \cdot t_{u, d}^b(k_d), \end{aligned} \quad (17)$$

where $\mathcal{V}(b, u, d, k)$ is the set of vehicles that have behavior b ($b \in B$) at time step k in link (u, d) , $\mathcal{K}(d, k_d)$ is the set of time steps k such that $kT \in [c_d \cdot k_d, c_d \cdot (k_d + 1)]$ at which the vehicles are in behavior b in link (u, d) , $E_{\theta, u, d}^b(k_d)$ is the constant traffic emission for emission θ of a vehicle on link (u, d) with behavior b during time period $[c_d \cdot k_d, c_d \cdot (k_d + 1)]$, $N_{u, d}^b(k_d)$ is the number of vehicles that have behavior b in link (u, d) during time period $[c_d \cdot k_d, c_d \cdot (k_d + 1)]$, and $t_{u, d}^b(k_d)$ is the length of the time period that the vehicles keep having this behavior.

Urban traffic states on a link can be separated into different scenarios according to the level of the traffic density. In the saturated traffic scenario, the queues of vehicles resulting from the red phase cannot be dissolved completely at the following green phase, i.e. all the arriving vehicles have to stop and wait once for the next green light to leave the link. For the over-saturated traffic scenario, the vehicles need to wait for even more cycle times in the queues than in saturated scenario. On the contrary, in the under-saturated traffic scenario, all the accumulated vehicles during the red phase are able to leave the link in the following green phase, some vehicles can even leave the link without any stop. Since the traffic behaviors could differ between these scenarios, the VT-S model can be further illustrated for the three scenarios.

1) *Saturated scenario*: In the saturated scenario, not all the vehicles waiting and arriving in the queues could leave the link in the current green phase, some vehicles have to wait until the next green phase, i.e. the number of vehicles waiting and arriving to leave the link exceeds the maximum number of vehicles that could leave at most in one cycle time, but the queues can be dissolved in the current green phase. This is characterized by the following condition:

$$\begin{aligned} q_{u, d}(k_d) &\leq \sum_{o \in O_{u, d}} \beta_{u, d, o}(k_d) \cdot \mu_{u, d} \cdot g_{u, d, o}(k_d) \\ &\leq c_d \cdot \alpha_{u, d}^{\text{arriv}}(k_d) + q_{u, d}(k_d). \end{aligned} \quad (18)$$

So, all the vehicles have to wait once for a red traffic signal in the queues before leaving the link, i.e. no vehicle can leave the link without a stop. For the saturated scenario, the number of vehicles that have behavior $b \in B$ in link (u, d) during time period $[c_d \cdot k_d, c_d \cdot (k_d + 1)]$ is given by

$$N_{u, d}^{\text{free}}(k_d) = n_{u, d}(k_d) - c_d \cdot \alpha_{u, d}^{\text{arriv}}(k_d) - q_{u, d}(k_d) \quad (19)$$

$$\begin{aligned} N_{u, d}^{\text{idling}, 1}(k_d) &= c_d \cdot \alpha_{u, d}^{\text{arriv}}(k_d) + q_{u, d}(k_d) - \\ &\quad \sum_{o \in O_{u, d}} \beta_{u, d, o}(k_d) \cdot \mu_{u, d} \cdot g_{u, d, o}(k_d) \end{aligned} \quad (20)$$

$$N_{u, d}^{\text{idling}, 2}(k_d) = \sum_{o \in O_{u, d}} \beta_{u, d, o}(k_d) \cdot \mu_{u, d} \cdot g_{u, d, o}(k_d) - q_{u, d}(k_d) \quad (21)$$

$$N_{u, d}^{\text{idling}, 3}(k_d) = 0 \quad (22)$$

$$N_{u, d}^{\text{idling}, 4}(k_d) = q_{u, d}(k_d) \quad (23)$$

$$N_{u, d}^{\text{dec}}(k_d) = c_d \cdot \alpha_{u, d}^{\text{arriv}}(k_d) \quad (24)$$

$$N_{u, d}^{\text{acc}}(k_d) = \sum_{o \in O_{u, d}} \beta_{u, d, o}(k_d) \cdot \mu_{u, d} \cdot g_{u, d, o}(k_d) \quad (25)$$

$$N_{u, d}^{\text{nonstop}}(k_d) = 0 \quad (26)$$

$$\begin{aligned} N_{u, d}^{\text{sns}}(k_d) &= c_d \cdot \alpha_{u, d}^{\text{arriv}}(k_d) + q_{u, d}(k_d) - \\ &\quad \sum_{o \in O_{u, d}} \beta_{u, d, o}(k_d) \cdot \mu_{u, d} \cdot g_{u, d, o}(k_d), \end{aligned} \quad (27)$$

and the length of the time periods that the vehicles keep having this behavior during time period $[c_d \cdot k_d, c_d \cdot (k_d + 1)]$ are

$$t_{u, d}^{\text{free}}(k_d) = c_d \quad (28)$$

$$t_{u, d}^{\text{idling}, 1}(k_d) = c_d - (v_{\text{low}} - v_{\text{free}})/a_{\text{dec}} \quad (29)$$

$$t_{u, d}^{\text{idling}, 2}(k_d) = c_d - (v_{\text{low}} - v_{\text{free}})/a_{\text{dec}} - (v_{\text{free}} - v_{\text{low}})/a_{\text{acc}} \quad (30)$$

$$t_{u, d}^{\text{idling}, 3}(k_d) = 0 \quad (31)$$

$$t_{u, d}^{\text{idling}, 4}(k_d) = c_d - (v_{\text{free}} - v_{\text{low}})/a_{\text{acc}} \quad (32)$$

$$t_{u, d}^{\text{dec}}(k_d) = (v_{\text{low}} - v_{\text{free}})/a_{\text{dec}} \quad (33)$$

$$t_{u, d}^{\text{acc}}(k_d) = (v_{\text{free}} - v_{\text{low}})/a_{\text{acc}} \quad (34)$$

$$t_{u, d}^{\text{nonstop}}(k_d) = 0 \quad (35)$$

$$t_{u, d}^{\text{sns}}(k_d) = (v_{\text{low}} - v_{\text{sns}})/a_{\text{dec}} + (v_{\text{sns}} - v_{\text{low}})/a_{\text{acc}}. \quad (36)$$

In the saturated scenario, equation (19) gives the number of vehicles that are running on link (u, d) with free-flow speed during the time period shown in (28). Equation (20) gives the number of vehicles that arrive at the end of the queues and decelerate to a low speed in link (u, d) , and then keep idling for the time period as in (29). Equation (21) gives the number of vehicles that decelerate to arrive at the end of the queues, keep idling for time period in (30), and then accelerate to leave link (u, d) . Equation (23) gives the number of vehicles in the queues that keep idling for the time period as in (32), and finally accelerate and leave link (u, d) . All the vehicles arriving at the end of the queues need to decelerate as (24) shows, and all the vehicles leaving link (u, d) will accelerate as (25) shows. The waiting vehicles in (27) that cannot leave the link in the current time interval will start and then stop again to keep on waiting in queues.

2) *Over-saturated scenario*: In the over-saturated scenario, the vehicles waiting in the queues could not leave the link in the current green phase. Hence, the number of vehicles waiting in the queues to leave the link exceeds the maximum number of vehicles that could leave at most in one cycle time:

$$\sum_{o \in O_{u, d}} \beta_{u, d, o}(k_d) \cdot \mu_{u, d} \cdot g_{u, d, o}(k_d) < q_{u, d}(k_d). \quad (37)$$

For the over-saturated scenario, the number of vehicles having behavior $b \in B$ during $[c_d \cdot k_d, c_d \cdot (k_d + 1)]$ is

$$N_{u, d}^{\text{free}}(k_d) = n_{u, d}(k_d) - c_d \cdot \alpha_{u, d}^{\text{arriv}}(k_d) - q_{u, d}(k_d) \quad (38)$$

$$N_{u, d}^{\text{idling}, 1}(k_d) = c_d \cdot \alpha_{u, d}^{\text{arriv}}(k_d) \quad (39)$$

$$N_{u, d}^{\text{idling}, 2}(k_d) = 0 \quad (40)$$

$$N_{u,d}^{\text{idling},3}(k_d) = q_{u,d}(k_d) - \sum_{o \in O_{u,d}} \beta_{u,d,o}(k_d) \cdot \mu_{u,d} \cdot g_{u,d,o}(k_d) \quad (41)$$

$$N_{u,d}^{\text{idling},4}(k_d) = \sum_{o \in O_{u,d}} \beta_{u,d,o}(k_d) \cdot \mu_{u,d} \cdot g_{u,d,o}(k_d) \quad (42)$$

$$N_{u,d}^{\text{dec}}(k_d) = c_d \cdot \alpha_{u,d}^{\text{arriv}}(k_d) \quad (43)$$

$$N_{u,d}^{\text{acc}}(k_d) = \sum_{o \in O_{u,d}} \beta_{u,d,o}(k_d) \cdot \mu_{u,d} \cdot g_{u,d,o}(k_d) \quad (44)$$

$$N_{u,d}^{\text{nonstop}}(k_d) = 0 \quad (45)$$

$$N_{u,d}^{\text{sns}}(k_d) = c_d \cdot \alpha_{u,d}^{\text{arriv}}(k_d) + q_{u,d}(k_d) - \sum_{o \in O_{u,d}} \beta_{u,d,o}(k_d) \cdot \mu_{u,d} \cdot g_{u,d,o}(k_d), \quad (46)$$

and the length of the time periods that the vehicles keep having this behavior in link (u, d) are given by

$$t_{u,d}^{\text{free}}(k_d) = c_d \quad (47)$$

$$t_{u,d}^{\text{idling},1}(k_d) = c_d - (v_{\text{low}} - v_{\text{free}})/a_{\text{dec}} \quad (48)$$

$$t_{u,d}^{\text{idling},2}(k_d) = 0 \quad (49)$$

$$t_{u,d}^{\text{idling},3}(k_d) = c_d \quad (50)$$

$$t_{u,d}^{\text{idling},4}(k_d) = c_d - (v_{\text{free}} - v_{\text{low}})/a_{\text{acc}} \quad (51)$$

$$t_{u,d}^{\text{dec}}(k_d) = (v_{\text{low}} - v_{\text{free}})/a_{\text{dec}} \quad (52)$$

$$t_{u,d}^{\text{acc}}(k_d) = (v_{\text{free}} - v_{\text{low}})/a_{\text{acc}} \quad (53)$$

$$t_{u,d}^{\text{nonstop}}(k_d) = 0 \quad (54)$$

$$t_{u,d}^{\text{sns}}(k_d) = (v_{\text{low}} - v_{\text{sns}})/a_{\text{dec}} + (v_{\text{sns}} - v_{\text{low}})/a_{\text{acc}}. \quad (55)$$

Except for the ‘‘idling’’ behavior, all the above formulas are the same as in the saturated scenario. All the vehicles arriving at the end of the queues as shown in (39) will decelerate and be idling for time period (48). A part of the vehicles waiting in the queues as in (41) cannot leave link (u, d) , and will be idling for the entire cycle time. All the vehicles as shown in (42) will be idling for time period (51), and then accelerate and leave link (u, d) .

3) *Under-saturated scenario:* In the under-saturated scenario, the queues can be dissolved before the current green phase ends. Thus, the traffic demand, i.e. the number of vehicles waiting and arriving to leave the link is less than the maximum number of vehicles that could leave in one cycle time, which is characterized as

$$c_d \cdot \alpha_{u,d}^{\text{arriv}}(k_d) + q_{u,d}(k_d) < \sum_{o \in O_{u,d}} \beta_{u,d,o}(k_d) \cdot \mu_{u,d} \cdot g_{u,d,o}(k_d). \quad (56)$$

Therefore, during a green phase, the vehicles waiting in the queues can be considered to first leave the link according to the saturated flow rate of the link $\mu_{u,d}$, and then, after the queues are dissolved, the arriving vehicles will leave the link without a stop according to the arriving (or demand) flow rate $\alpha_{u,d}^{\text{arriv}}(k_d)$ in the rest of the green time. Hereafter, the green time for link (u, d) in the k_d th cycle time, $g_{u,d}(k_d)$, can be approximately separated into two parts, one is the green time $g_{u,d}^s(k_d)$ in which the traffic leaves the link with the saturated flow rate, the other is the green time $g_{u,d}^d(k_d)$ during which the

traffic leaves the link with the demand flow rate. The quantities $g_{u,d}^s(k_d)$ and $g_{u,d}^d(k_d)$ satisfy

$$\begin{aligned} c_d \alpha_{u,d}^{\text{arriv}}(k_d) + q_{u,d}(k_d) &= g_{u,d}^s(k_d) \mu_{u,d} + g_{u,d}^d(k_d) \alpha_{u,d}^{\text{arriv}}(k_d) \\ g_{u,d}^s(k_d) + g_{u,d}^d(k_d) &= g_{u,d}(k_d). \end{aligned} \quad (57)$$

Hence, we have

$$g_{u,d}^s(k_d) = \frac{c_d \alpha_{u,d}^{\text{arriv}}(k_d) + q_{u,d}(k_d) - g_{u,d}(k_d) \alpha_{u,d}^{\text{arriv}}(k_d)}{\mu_{u,d} - \alpha_{u,d}^{\text{arriv}}(k_d)} \quad (58)$$

$$g_{u,d}^d(k_d) = \frac{g_{u,d}(k_d) \mu_{u,d} - c_d \alpha_{u,d}^{\text{arriv}}(k_d) - q_{u,d}(k_d)}{\mu_{u,d} - \alpha_{u,d}^{\text{arriv}}(k_d)}. \quad (59)$$

For the under-saturated scenario, the number of vehicles that have behavior $b \in B$ in link (u, d) [$c_d \cdot k_d, c_d \cdot (k_d + 1)$] is

$$N_{u,d}^{\text{free}}(k_d) = n_{u,d}(k_d) - c_d \cdot \alpha_{u,d}^{\text{arriv}}(k_d) - q_{u,d}(k_d) \quad (60)$$

$$N_{u,d}^{\text{idling},1}(k_d) = 0 \quad (61)$$

$$N_{u,d}^{\text{idling},2}(k_d) = (c_d - g_{u,d}^d(k_d)) \alpha_{u,d}^{\text{arriv}}(k_d) \quad (62)$$

$$N_{u,d}^{\text{idling},3}(k_d) = 0 \quad (63)$$

$$N_{u,d}^{\text{idling},4}(k_d) = q_{u,d}(k_d) \quad (64)$$

$$N_{u,d}^{\text{dec}}(k_d) = (c_d - g_{u,d}^d(k_d)) \alpha_{u,d}^{\text{arriv}}(k_d) \quad (65)$$

$$N_{u,d}^{\text{acc}}(k_d) = g_{u,d}^s(k_d) \mu_{u,d} \quad (66)$$

$$N_{u,d}^{\text{nonstop}}(k_d) = g_{u,d}^d(k_d) \alpha_{u,d}^{\text{arriv}}(k_d) \quad (67)$$

$$N_{u,d}^{\text{sns}}(k_d) = 0, \quad (68)$$

and the time periods that the vehicles keep having this behavior in link (u, d) are given by

$$t_{u,d}^{\text{free}}(k_d) = c_d \quad (69)$$

$$t_{u,d}^{\text{idling},1}(k_d) = 0 \quad (70)$$

$$t_{u,d}^{\text{idling},2}(k_d) = c_d - g_{u,d}^d(k_d) - (v_{\text{low}} - v_{\text{free}})/a_{\text{dec}} \quad (71)$$

$$- (v_{\text{free}} - v_{\text{low}})/a_{\text{acc}} \quad (72)$$

$$t_{u,d}^{\text{idling},3}(k_d) = 0 \quad (73)$$

$$t_{u,d}^{\text{idling},4}(k_d) = c_d - g_{u,d}^d(k_d) - (v_{\text{free}} - v_{\text{low}})/a_{\text{acc}} \quad (74)$$

$$t_{u,d}^{\text{dec}}(k_d) = (v_{\text{low}} - v_{\text{free}})/a_{\text{dec}} \quad (75)$$

$$t_{u,d}^{\text{acc}}(k_d) = (v_{\text{free}} - v_{\text{low}})/a_{\text{acc}} \quad (76)$$

$$t_{u,d}^{\text{nonstop}}(k_d) = \begin{cases} (v_{\text{agg}} - v_{\text{free}})/a_{\text{acc}} & \text{if } O \leq \lambda \\ (v_{\text{con}} - v_{\text{free}})/a_{\text{dec}} & \text{if } O > \lambda \end{cases} \quad (77)$$

$$t_{u,d}^{\text{sns}}(k_d) = 0. \quad (78)$$

In the under-saturated scenario, no vehicle will be held at the stop-line for more than one cycle time, i.e. all the queues will be dissolved in the following green time. Thus, only ‘‘idling,2’’ and ‘‘idling,4’’ vehicles exist. All the arriving vehicles except the ‘‘nonstop’’ vehicles (as in (62)) will experience deceleration and acceleration, and be idling for the time period in (72). All the waiting vehicles in the queues in (64) will be idling for the time period (74), and then accelerate to leave the link. Only the arriving vehicles except the vehicles that do not need to stop will decelerate and wait in queues as in (65). All the vehicles leaving at the saturation flow rate have to accelerate to leave the link as (66) shows. The arriving vehicles as shown

in (67) will leave link (u, d) with acceleration or deceleration (depending on the capacity occupancy rate of the link) without stops.

V. MPC FOR URBAN TRAFFIC NETWORKS

Model Predictive Control [21] is a methodology that implements and repeatedly applies Optimal Control in a rolling horizon way. The aforementioned integrated VT-S model is able to efficiently predict both the traffic flows and the traffic emissions, which can be used to compute the control performance, and thus the VT-S model can be used as the prediction model of the MPC controller.

Based on the prediction model, at every control time step, an optimization problem needs to be solved on-line over a prediction horizon to derive the sequence of the optimal future control decisions. Solving this optimization problem is the key part of the MPC methodology, and is also the step that costs most of the on-line computation. Given the control time interval T_{ctrl} and the simulation time interval c_d of node $d \in J$, there exists an integer N_d such that

$$T_{\text{ctrl}} = N_d c_d, \quad (79)$$

according to the definition of the cycle times for the nodes in a traffic network, as shown in (7). For a given k_d , the corresponding value of k_{ctrl} is given by

$$k_{\text{ctrl}}(k_d) = \left\lfloor \frac{k_d}{N_d} \right\rfloor, \quad (80)$$

where $\lfloor x \rfloor$ for x a real number denotes the largest integer less than or equal to x . On the other hand, a given value k_{ctrl} of the control time step corresponds to the set $\{k_{\text{ctrl}}N_d, k_{\text{ctrl}}N_d + 1, \dots, (k_{\text{ctrl}} + 1)N_d - 1\}$ of simulation time steps.

When the prediction horizon is N_p , the optimization problem of MPC can be expressed as

$$\begin{aligned} \min_{\mathbf{g}(k_{\text{ctrl}})} J &= J(k_{\text{ctrl}}) \\ \text{s.t.} \quad &\text{VT-S model} \\ &\Phi(\mathbf{g}(k_{\text{ctrl}})) = 0 \\ &g_{\min} \leq \mathbf{g}(k_{\text{ctrl}}) \leq g_{\max} \end{aligned} \quad (81)$$

where $\mathbf{g}(k_{\text{ctrl}})$ is the future control input at control step k_{ctrl} (e.g. the green times), i.e. $\mathbf{g}(k_{\text{ctrl}}) = [g^T(k_{\text{ctrl}}|k_{\text{ctrl}}) \ g^T(k_{\text{ctrl}} + 1|k_{\text{ctrl}}) \ \dots \ g^T(k_{\text{ctrl}} + N_p - 1|k_{\text{ctrl}})]^T$, and the vector $g(k_{\text{ctrl}} + j|k_{\text{ctrl}})$ denotes the control input at the j th control step in the future based on information at the current control time step k_{ctrl} . The equality constraint in (81) is the cycle time constraint, i.e. the sum of the green times of all the phases equals to the cycle time in an intersection. To decrease the on-line computational complexity, a control horizon N_c ($N_c < N_p$) can be defined, such that $g(k_{\text{ctrl}} + i|k_{\text{ctrl}}) = g(k_{\text{ctrl}} + N_c - 1|k_{\text{ctrl}})$ for $i = N_c, \dots, N_p - 1$. This nonlinear optimization problem can be solved by e.g. multi-start Sequential Quadratic Programming (SQP) algorithm [25, Chapter 5].

The objective function of the integrated urban control problem at control time step k_{ctrl} is

$$J(k_{\text{ctrl}}) = \sum_{\theta \in \Theta} \frac{\lambda_{\theta}}{E_{\theta, \text{nominal}}} \sum_{(u,d) \in L} \sum_{k_d=N_d k_{\text{ctrl}}+1}^{N_d(k_{\text{ctrl}}+N_p)} E_{\theta, u,d}(k_d), \quad (82)$$

where $E_{\theta, u,d}(k_d)$ denotes the estimated partial criterion for θ in link (u, d) at simulation time step k_d , $\Theta = \{\text{TTS}, \text{CO}, \text{NO}_x, \text{HC}\}$ is the set of the control objectives, $E_{\theta, \text{nominal}}$ is the nominal performance for objective $\theta \in \Theta$ to normalize the partial objective of θ , and λ_{θ} is the weight parameter for objective θ . For the Total Time Spent (TTS), we have

$$E_{\text{TTS}, u,d}(k_d) = T_{\text{sim}} \cdot n_{u,d}(k_d), \quad (83)$$

where $n_{u,d}(k_d)$ is derived by (1), T_{sim} is the simulation time step of the VT-S model, and (17) will be used for computing emissions. The goal of the control problem is to reduce the combined performance of the Total Time Spent and the variety of traffic emissions (i.e. CO, NO_x, and HC) of the whole urban traffic network over the entire prediction horizon. Hence, it turns out to be a multiple objective control problem. By changing the weights of the objective function, a different emphasis can be assigned for different kinds of control purposes.

Once the optimal control input sequence $\mathbf{g}^*(k_{\text{ctrl}})$ is determined by the optimization, the first sample of the optimal results, $g^*(k_{\text{ctrl}} | k_{\text{ctrl}})$, is implemented in the urban traffic network. When arriving to the next control step, the prediction model is fed with the newly measured traffic states (i.e. the number of vehicles on a link [26]), the whole prediction horizon is shifted one step forward, and the optimization starts over again. By operating the on-line optimization in the receding horizon way, the MPC controller closes the control loop, and enables the system to get feedback from the real traffic network, which makes the controller adaptive to the uncertainties and disturbances caused by model mismatches and errors in the external demand prediction.

VI. SIMULATIONS

We use CORSIM [27] to simulate the real traffic environment, and design MPC controllers to decide control inputs for the traffic signals in CORSIM. The simulated urban road subnetwork is shown in Fig. 3. Nodes marked as ‘‘Sx’’ are the source nodes where traffic flows enter and leave the network.

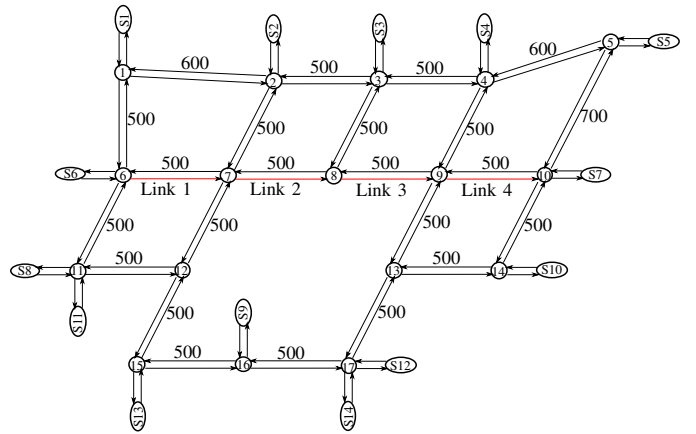


Fig. 3. An urban traffic network

MPC controllers for urban traffic are designed to reduce both TTS and TE (Total Emissions for CO, NO_x, and HC) for this urban traffic network. MPC controllers are designed

based on the weights specified for the different objectives, as shown in Table I.

TABLE I
COMBINATION OF WEIGHT PARAMETERS FOR THE MULTI-OBJECTIVE MPC CONTROLLERS

MPC	λ_{TTS}	λ_{CO}	λ_{NO_x}	λ_{HC}
TTS	1	0	0	0
TE	0	0.33	0.33	0.34
TTS+TE	0.5	0.16	0.17	0.17

In the traffic network shown in Fig. 3, the lengths of the roads are indicated in meter. Each of the roads in the traffic network has 3 lanes, and the turning rates for each link are all the same, i.e. left turn 33%, through turn 34%, right turn 33%. The storage capacities of the links are fixed according to the link lengths, the number of lanes, and the average vehicle length (7 m). The free-flow speed is 50 km/h. The simulations run for 80 min, and the traffic demands of all the source nodes (i.e. network inflows) are given in Fig. 4.

For the set-up of the traffic controllers of this network, the cycle time is set to 60s for all the intersections, except 30s for Intersection 8. During the experiments, the simulation time intervals are set to equal to the cycle times of every intersection. For the MPC controllers, the control time interval T_{ctrl} is 120s, the prediction horizon N_p is 5, and the control horizon is set to $N_c = N_p$. The results of MPC controllers are compared with that of a fixed-time strategy. The fixed-time control strategy is defined having constant phases, cycle times, green time durations, and the offsets. The fixed-time signals are determined based on the data for the saturated scenario, i.e. the green times are proportional to the traffic demands from each direction, which depend on the saturated flow rates and the turning rates under the saturated scenario [22], [28].

The performance indicators that CORSIM provides to evaluate the effect of the controllers include the TTS, the TE for CO, NO_x , and HC respectively, the mean speed, the number of stops, etc. The results for each control performance are illustrated in Table II for the different control strategies. As Table II shows, the MPC controllers are able to reduce the objectives, including TTS and the TE for CO, NO_x , and HC, compared to the FT controller. The TTS-based MPC and the TE-based MPC are MPC controllers taking only the TTS or only the TE of the whole network as control objective respectively. For the TTS-based MPC, the TTS is reduced obviously, but its ability for reduction of the TE is quite limited, where the emissions for HC even increase. For the TE-based MPC, the TE for each of the gases is reduced, but the TTS becomes higher than the TTS-based MPC. When both the TTS and the TE are considered for the control objective as in the TTS+TE-based MPC, a trade-off is made to balance the TTS and the TE. The TE-based MPC is able to increase the mean speed and to reduce the number of stops for the traffic network, so as to obtain smoother traffic flows. The TTS-based MPC can also improve the mean speed of the traffic network, but at the cost of increasing the stop-and-go behavior and the vehicular emissions. The improvements made by the MPC controllers also illustrate the adaptiveness of MPC to the uncertainties and disturbances caused by model mismatches

and errors in the external demand prediction.

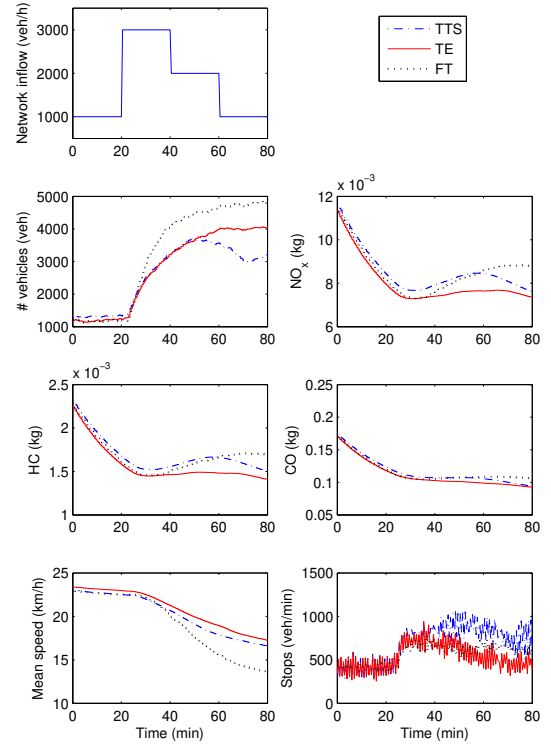


Fig. 4. Evolution of the traffic states for the traffic network in the implemented urban network

In urban traffic networks, traffic flows with fewer stops, shorter delays, and moderate speed will release less emissions [17]. In Fig. 4, we demonstrate the evolution of some traffic states for the entire traffic network in Fig. 3, including the number of vehicles, the emissions for CO, NO_x , and HC, the mean speed, and the number of stops per minute. As the figure shows, the TE-based MPC controller obtains higher network mean speeds and fewer number of stops compared to the TTS-based MPC controller, which results in smoother traffic flows within the traffic network. Consequently, TE-based MPC is able to keep the total emissions from increasing when the network inflow grows. On the contrary, TTS-based MPC successfully reduces the number of vehicles in the traffic network, but it is not good at regulating emissions.

Fig. 5 and 6 illustrate the evolution of the traffic states for Link 2 and Link 3 in the network of Fig. 3. The results of the Fixed-time controller (FT), the TTS-based MPC, and the TE-based MPC are compared in the figures. At the start of the simulation, all the emissions are high in both links, because at the beginning of the simulation, the traffic network is empty and the network inflows are low, so vehicles tend to accelerate more and made fewer stops until the traffic flows reach an equilibrium or the network inflows increase. When the number of vehicles grows with the network inflow in the links (i.e. the links become more crowded), we can see that the mean speed decreases and the number of stops increases, thereafter, more emissions are released for the different kinds of gases. In Fig. 5, the TE-based MPC has a good effect on reducing

TABLE II
PERFORMANCE COMPARISON OF TTS AND TE FOR A FIXED-TIME CONTROLLER (FT) AND FOR THE MPC CONTROLLERS WITH VARIOUS OBJECTIVE FUNCTIONS (SEE TABLE I)

Controller	TTS (veh-h)	TE (kg)			Mean Speed (veh/h)	Stops (veh/min)
		CO	NO _x	HC		
FT	1.58×10^7	18.5668	1.3605	0.2674	19.13	568
TE	1.34×10^7 (-15.19%)	17.7603 (-4.34%)	1.2774 (-6.11%)	0.2511 (-6.10%)	20.85 (8.99%)	540 (-4.93%)
TTS	1.26×10^7 (-20.25%)	18.5332 (-0.18%)	1.3600 (-0.04%)	0.2690 (0.60%)	20.20 (5.59%)	693 (22.01%)
TTS+TE	1.31×10^7 (-17.09%)	18.1040 (-2.49%)	1.2932 (-4.95%)	0.2539 (-5.05%)	20.60 (5.63%)	549 (-3.35%)

The data in parenthesis are the relative change for each performance indicator compared with that of the FT controller

all kinds of emissions, when the traffic density grows. But the emission mitigation ability of the TTS-based MPC is not better than that of the FT controller in Link 2. The emission mitigation ability of the TE-based MPC is confirmed again for Link 3 in Fig. 6, where the mean speed is more stable and the number of stops is obviously smaller. Fig. 7 illustrates the variation of the mean speed over time on Link 1, 2, 3, and 4 (see Fig. 3 for the locations of the links). More specifically, Fig. 7(a) gives the results for the FT controller, Fig. 7(b) for the TE-based MPC controller, and Fig. 7(c) for the TTS-based MPC controller. We can see from the figures that the values of the mean speed under the MPC controllers are kept higher and

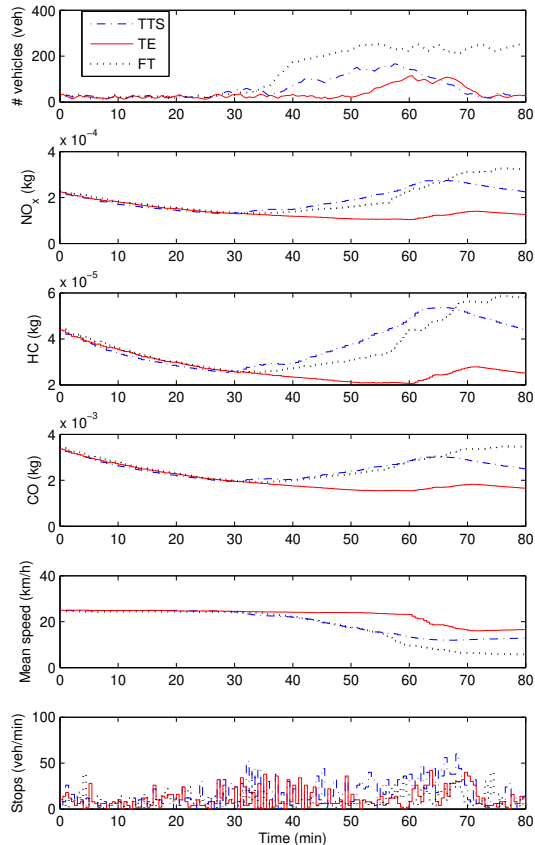


Fig. 5. Evolution of the traffic states for Link 2

As Table II illustrates, since the MPC controllers focus on different control objectives, TTS-based MPC can reduce the

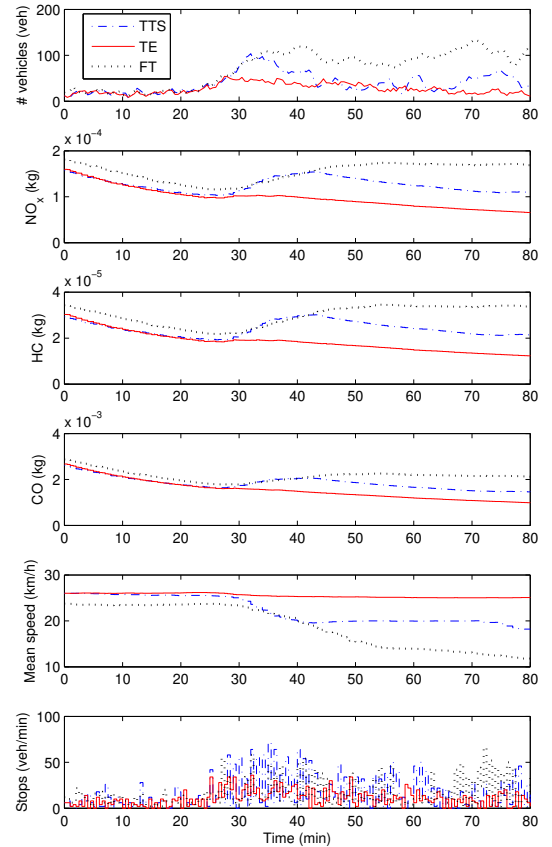


Fig. 6. Evolution of the traffic states for Link 3

TTS more than TE-based MPC; and on the contrary, TE-based MPC is able to reduce the TE more than TTS-based MPC. A trade-off between the TTS and TE can be obtained by integrating the two control objectives. For freeway traffic, the speed range of vehicles is normally from 0 km/h to 120 km/h, in which range the vehicles will release comparatively high emissions when the speed of vehicles is either very low or very high. Thus, the TTS performance conflicts with the TE performance, when the speed of vehicles grows high [19]. However, for urban traffic, due to the speed limit (normally 60 km/h), a high speed is not an important cause for high emissions anymore, but the stop-and-go driving behavior is the main cause of generating emissions. Therefore, for urban traffic emission reduction, we need to focus on smoothing traffic flows and decreasing the number of accelerations and

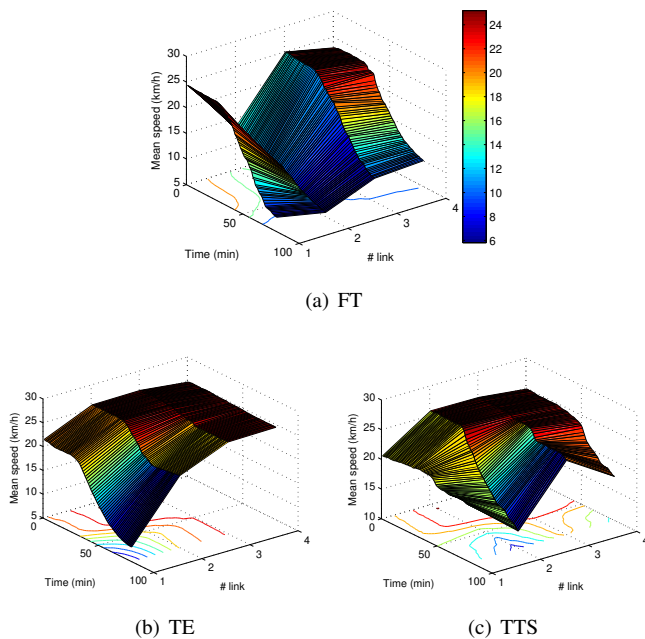


Fig. 7. The mean speed on the links for (a) the FT controller, (b) the TE-based MPC controller, and (c) the TTS-based MPC controller

stops. TTS, i.e. the sum of total travel time and total delay time, is a performance aiming at controlling the traveling efficiency. By using the integrated traffic flow and vehicle emission model, the TE control objective focuses on not only traveling efficiency, but also considers the stop-and-go behavior. The TE-based MPC controller is able to reduce all kinds of traffic emissions for the links and for the entire network, and at the same time, to keep a more steady vehicle density on the links, smoother traffic flows and mean speeds, and a lower number of stops. The TTS-based MPC aims at reducing the TTS of traffic network by regulating the stop-and-go behavior and partitions of traffic flows within the network with the aid of traffic signals. To achieve a lower TTS, the TTS-based MPC obtained higher number of stops than the FT controller.

VII. CONCLUSION

An integrated macroscopic urban traffic flow and emission model, the VT-S model, is proposed for urban traffic MPC controller. The VT-S model is able to predict the traffic flow states, as well as the emissions released by every vehicle at different operational conditions, i.e. the speed and the acceleration. This model enables the MPC controller to address control problems with multiple objectives, i.e. reducing both travel delays and traffic emissions.

Based on the VT-S model, the MPC controller can successfully reduce both the total emissions and the total time spent of urban traffic networks by specifying the control performance indicator. The TTS-based MPC and the TE-based MPC take the total time spent and the total emissions as the control objectives respectively. The TTS-based MPC performs better in decreasing the total time spent at a cost of releasing more traffic emissions; the TE-based MPC decreases the total

emission level obviously, but its ability in reducing the total time spent is restricted. The MPC based on both control objectives achieves a trade-off between the total time spent and the total emissions of the traffic network. By applying the total emissions as the control objective, the MPC controller can not only reduce the traffic emissions of urban traffic networks, but also keep a comparatively smoother traffic flow mean speed and less vehicle stops.

In the future, we will extend the VT-S model into a multi-class model to describe the emissions of different types of vehicles, and also consider the surrounding traffic dynamics, then further evaluate the proposed model-based controller for reducing fuel consumption and CO₂ emission for urban traffic networks. Moreover, we will calibrate the model and implement the proposed model-based controller in a real-life traffic network, and further assess its control effect.

ACKNOWLEDGMENT

This research is supported by the National Science Foundation of China (60934007, 61104160, 61203169), Shanghai Education Council Innovation Research Project (12ZZ024), Chinese International Cooperation Project of National Science Committee (Grant No. 71361130012), the European COST Actions TU0702 and TU1102, the BSIK project “Next Generation Infrastructures (NGI)”, and the Transport Research Centre Delft.

REFERENCES

- [1] A. Nagurney, “Congested urban transportation networks and emission paradoxes,” *Transportation Research Part D: Transport and Environment*, vol. 5, no. 2, pp. 145–151, 2000.
- [2] P. Lowrie, “The Sydney coordinated adaptive traffic system: principles, methodology, algorithms,” in *Proceedings of the International Conference on Road Traffic Signalling*, Mar. 1982, pp. 67–70.
- [3] D. Robertson and R. Bretherton, “Optimizing networks of traffic signals in real time - The SCOOT method,” *IEEE Transactions on Vehicular Technology*, vol. 40, no. 1, pp. 11–15, 1991.
- [4] A. Hegyi, B. De Schutter, and J. Hellendoorn, “Optimal coordination of variable speed limits to suppress shock waves,” *IEEE Transactions on Intelligent Transportation Systems*, vol. 6, no. 1, pp. 102–112, Mar. 2005.
- [5] K. Aboudolas, M. Papageorgiou, A. Kouvelas, and E. Kosmatopoulos, “A rolling-horizon quadratic-programming approach to the signal control problem in large-scale congested urban road networks,” *Transportation Research Part C: Emerging Technologies*, vol. 18, no. 5, pp. 680–694, 2010.
- [6] S. Lin, B. De Schutter, Y. Xi, and H. Hellendoorn, “Fast model predictive control for urban road networks via MILP,” *IEEE Transactions on Intelligent Transportation Systems*, vol. 12, no. 3, pp. 846–856, Sep. 2011.
- [7] R. Carlson, I. Papamichail, and M. Papageorgiou, “Local feedback-based mainstream traffic flow control on motorways using variable speed limits,” *IEEE Transactions on Intelligent Transportation Systems*, vol. 12, no. 4, pp. 1261–1276, 2011.
- [8] A. Kouvelas, K. Aboudolas, E. Kosmatopoulos, and M. Papageorgiou, “Adaptive performance optimization for large-scale traffic control systems,” *IEEE Transactions on Intelligent Transportation Systems*, vol. 12, no. 4, pp. 1434–1445, 2011.
- [9] L. Baskar, B. De Schutter, and H. Hellendoorn, “Traffic management for automated highway systems using model-based predictive control,” *IEEE Transactions on Intelligent Transportation Systems*, vol. 13, no. 2, pp. 838–847, 2012.
- [10] M. K. Ekbatani, A. Kouvelas, I. Papamichail, and M. Papageorgiou, “Exploiting the fundamental diagram of urban networks for feedback-based gating,” *Transportation Research Part B: Methodological*, vol. 46, no. 10, pp. 1393 – 1403, 2012.

- [11] —, “Congestion control in urban networks via feedback gating,” *Procedia - Social and Behavioral Sciences*, vol. 48, no. 17, pp. 1599–1610, 2012.
- [12] N. Geroliminis, J. Haddad, and M. Ramezani, “Optimal perimeter control for two urban regions with macroscopic fundamental diagrams: A model predictive approach,” *IEEE Transactions on Intelligent Transportation Systems*, vol. 14, no. 1, pp. 348–359, Mar. 2013.
- [13] B. Asadi and A. Vahidi, “Predictive cruise control: Utilizing upcoming traffic signal information for improving fuel economy and reducing trip time,” *IEEE Transactions on Control Systems Technology*, vol. 19, no. 3, pp. 707–714, 2011.
- [14] M. Kamal, M. Mukai, J. Murata, and T. Kawabe, “Ecological vehicle control on roads with up-down slopes,” *IEEE Transactions on Intelligent Transportation Systems*, vol. 12, no. 3, pp. 783–794, 2011.
- [15] M. Ferreira and P. D’Orey, “On the impact of virtual traffic lights on carbon emissions mitigation,” *IEEE Transactions on Intelligent Transportation Systems*, vol. 13, no. 1, pp. 284–295, 2012.
- [16] C. Li and S. Shimamoto, “Dynamic traffic light control scheme for reducing CO2 emissions employing ETC technology,” *International Journal of Managing Public Sector Information and Communication Technologies*, vol. 2, no. 1, 2011.
- [17] A. Stevanovic, J. Stevanovic, K. Zhang, and S. Batterman, “Optimizing traffic control to reduce fuel consumption and vehicular emissions,” *Transportation Research Record: Journal of the Transportation Research Board*, pp. 105–113, 2009.
- [18] S. Zegeye, B. De Schutter, H. Hellendoorn, E. Breunese, and A. Hegyi, “Integrated macroscopic traffic flow, emission, and fuel consumption model for control purposes,” *Transportation Research Part C: Emerging Technologies*, 2012, in press.
- [19] S. Zegeye, B. De Schutter, H. Hellendoorn, and E. Breunese, “Model-based traffic control for balanced reduction of fuel consumption, emissions, and travel time,” in *Proceedings of the 12th IFAC Symposium on Transportation Systems*, Redondo Beach (CA), USA, Sep. 2009, pp. 149–154.
- [20] M. Ferreira, R. Fernandes, H. Conceição, W. Viriyasitavat, and O. Tonguz, “Self-organized traffic control,” in *Proceedings of the seventh ACM international workshop on VehiculAr InterNETworking*. ACM, 2010, pp. 85–90.
- [21] J. Rawlings and D. Mayne, *Model Predictive Control: Theory and Design*. Madison, Wisconsin: Nob Hill Publishing, 2009.
- [22] S. Lin, B. De Schutter, Y. Xi, and H. Hellendoorn, “Efficient network-wide model-based predictive control for urban traffic networks,” *Transportation Research Part C: Emerging Technologies*, vol. 24, pp. 122–140, Oct. 2012.
- [23] K. Ahn, H. Rakha, A. Trani, and M. Van Aerde, “Estimating vehicle fuel consumption and emissions based on instantaneous speed and acceleration levels,” *Journal of Transportation Engineering*, vol. 128, no. 2, pp. 182–190, 2002.
- [24] S. Zegeye, B. De Schutter, H. Hellendoorn, and E. Breunese, “Reduction of travel times and traffic emissions using model predictive control,” in *Proceedings of the 2009 American Control Conference*, St. Louis (MO), USA, Jun. 2009, pp. 5392–5397.
- [25] P. Pardalos and M. Resende, Eds., *Handbook of Applied Optimization*. Oxford, UK: Oxford University Press, 2002.
- [26] M. Papageorgiou and G. Vigos, “Relating time-occupancy measurements to space-occupancy and link vehicle-count,” *Transportation Research Part C: Emerging Technologies*, vol. 16, no. 1, pp. 1–17, 2008.
- [27] FHWA, *Traffic Software Integrated System Version 5.1 User’s Guide*, 2001.
- [28] M. Papageorgiou, *Applications of Automatic Control Concepts to Traffic Flow Modeling and Control*. Springer-Verlag New York, Inc. Secaucus, NJ, USA, 1983.